BR9431715

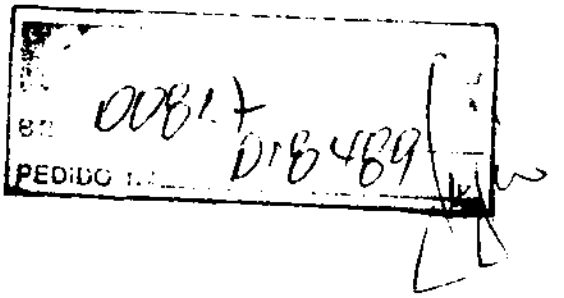

INPE-4621 (PRE--1342)

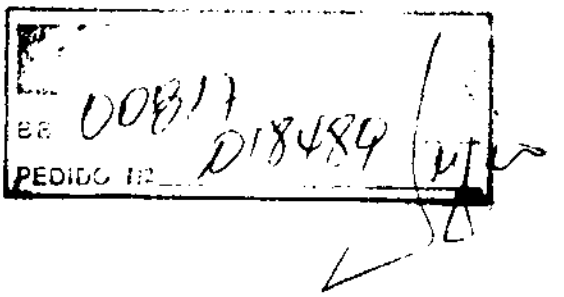

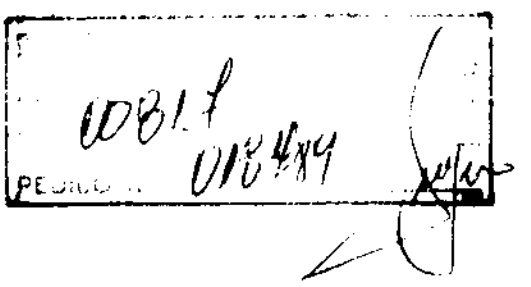

BR 9431715

1. Publication NO **INPE-4621-PRE/1342**	2. Version	3. Date **July, 1988**	5. Distribution ☐ Internal ☒ External ☐ Restricted
4. Origin *LAP*	Program *PION*		

6. Key words - selected by the author(s)

KINETIC EFFECTS
ION-ACOUSTIC NEGATIVE SOLITONS
PLASMA WITH NEGATIVE IONS

7. U.D.C.: **533.951.3**

8. Title **INPE-4621-PRE/1342**

KINETIC EFFECTS ON THE PROPAGATION CHARACTERISTICS OF ION ACOUSTIC NEGATIVE SOLITONS

10. NO of pages: *27*

11. Last page: *25*

12. Revised by

Abraham C.-L. Chian

9. Authorship

Marisa Roberto
Gerson Otto Ludwig
José Augusto Bittencourt

Responsible author *Marisa Roberto*

13. Authorized by

Marco Antonio Raupp
Director General

14. Abstract/Notes

The propagation characteristics of ion-acoustic negative solitons, in a multi-component plasma with negative ions, are investigated considering a kinetic model which takes into account electron reflection and positive ion trapping in the negative potential well of the soliton. The Poisson equation is solved consistently using the Sagdeev potential formalism. It is verified that the kinetic effects associated with trapping of positive ions and reflection of electrons modify the results predicted by the simple Korteweg-de Vries fluid model in such a way that the Mach numer is reduced as the ion temperature and the population of reflected electrons increase. Comparison with experimental observations shows that the measured values of the Mach number can be reproduced by this kinetic model under proper selection of the ion temperature and the shape of the reflected electron distribution function, with a dependence on the negative ion concentration.

15. Remarks

To be submitted for publication in Plasma Physics and Controlled Fusion.

KINETIC EFFECTS ON THE PROPAGATION CHARACTERISTICS OF ION-ACOUSTIC NEGATIVE SOLITONS

M. Roberto, C.O. Ludwig and J.A. Bittencourt

Instituto de Pesquisas Espaciais - INPE

Ministério da Ciência e Tecnologia - MCT

São José dos Campos, SP, 12225, Brazil

ABSTRACT

The propagation characteristics of ion-acoustic negative solitons, in a multi-component plasma with negative ions, are investigated considering a kinetic model which takes into account electron reflection and positive ion trapping in the negative potential well of the soliton. The Poisson equation is solved consistently using the Sagdeev potential formalism. It is verified that the kinetic effects associated with trapping of positive ions and reflection of electrons modify the results predicted by the simple Korteweg-de Vries fluid model in such a way that the Mach number is reduced as the ion temperature and the population of reflected electrons increase. Comparison with experimental observations shows that the measured values of the Mach number can be reproduced by this kinetic model under proper selection of the ion temperature and the shape of the reflected electron distribution function, with a dependence on the negative ion concentration.

1. INTRODUCTION

The ion-acoustic negative solitons, also referred to in the literature as rarefactive solitons, correspond to a propagating localized depression in the plasma potential resulting from a compression of negative ions in a multi-component plasma, whereas the ion-acoustic positive solitons are propagating positive potential pulses due to a compression of positive ions. The ion-acoustic positive solitons have been extensively investigated, using a fluid model, leading to the Korteweg-de Vries equation (e.g. Washimi and Taniuti, 1966; Ikezi et al., 1970; Sakanaka, 1972; Tran, 1979) and using a kinetic model, which included trapping of electrons in the soliton potential (e.g. Schamel, 1972; Schamel, 1973; Schamel, 1979). The ion-acoustic negative solitons have also been theoretical investigated using fluid models (e.g. Das and Tagare, 1975; Tagare, 1975).

The first experimental observations of ion-acoustic negative solitons were made in a double plasma machine (Ludwig et al., 1984) using a gas mixture of Ar and SF_6. Further experimental investigations were also made by Nakamura and Tsukabayashi (1984), and Nakamura et al. (1985a), using Ar and SF_6. The experimental results for the Mach number obtained by Nakamura et al. (1985a), agreed reasonably well with theoretical predictions of a fluid model, whereas those of Ludwig et al. (1984), using a smaller double-plasma device, indicated Mach numbers much larger than those predicted by a fluid model. These high Mach number values could not be explained on the basis of simple fluid models with isothermal electrons using the Korteweg-de Vries equation (Ludwig et al., 1984), or using the Sagdeev potential formalism (Nakamura et al., 1985b).

Also, inclusion of the finite ion temperature effect (pressure gradient term) in the fluid model did not alter significantly the Mach number values (Nakamura et al., 1985a). It seems, therefore, that kinetic effects, such as trapping of positive ions and reflection of electrons by the soliton negative potential well, may be important in the formulation of a theoretical model for ion-acoustic negative solitons.

In this paper the role played by kinetic effects on the propagation characteristics of ion-acoustic negative solitons is investigated. The kinetic model described here includes electron reflection and positive ion trapping in the negative potential well of the soliton, and uses the Sagdeev potential formalism (Sagdeev, 1966). This method can account for large amplitude solitons, whose experimental observation have already been reported (Nakamura et al., 1985b), whereas the Korteweg-de Vries equation method applies only to small amplitude solitons.

2. THEORETICAL MODEL

A multi-component plasma composed of hot electrons (mass m_e, charge -e), hot positive ions (mass m_+, charge e) and cold negative ions (mass m_-, charge -e) is considered. Position coordinates in the reference frames of the laboratory (x) and of the soliton (x') are related by $x' = x - ut$, where u denotes the soliton speed in the laboratory frame. The soliton negative potential $\phi(x')$ satisfies the one-dimensional Poisson equation

$$\frac{d^2\phi(x')}{d(x')^2} = -\frac{1}{\varepsilon_0}\rho(x') \quad , \tag{1}$$

where ϵ_0 is the free space electric permittivity and the total electric charge density $\rho(x')$ includes the contributions from electrons, $\rho_e(x')$, positive ions, $\rho_+(x')$ and negative ions, $\rho_-(x')$,

$$\rho(x') = \rho_e(x') + \rho_+(x') + \rho_-(x') \ . \tag{2}$$

The electric charge densities for the electrons and for the positive ions can be expressed in terms of their distribution functions $f_e(x',v)$ and $f_+(x',v)$, respectively,

$$\rho_a(x') = q_a \int_{-\infty}^{+\infty} f_a(x',v) d^3v \ , \tag{3}$$

with a = e, +, where $f_a(x',v)$ satisfies the time-independent Vlasov equation,

$$v \frac{\partial f_a}{\partial x'} - \frac{q_a}{m_a} \frac{d\phi}{dx'} \frac{\partial f_a}{\partial v} = 0 \ . \tag{4}$$

For the cold negative ions, $\rho_-(x') = -en_-(x')$, where the negative ion number density $n_-(x')$ is given by

$$n_-(x') = \frac{n_-^0}{[1 + 2e\phi(x')/m_- u^2]^{1/2}} \ , \tag{5}$$

obtained considering conservation of particle flux and of energy,

$$n_-(x')u_-(x') = n_-^0 u_-^0 \ , \tag{6}$$

$$\frac{1}{2} m_- u_-^2(x') - e\phi(x') = \frac{1}{2} m_- (u_-^0)^2 \ , \tag{7}$$

respectively. In these expressions $u_-(x')$ denotes the negative ion macroscopic velocity, and n_-^0 and u_-^0 are the negative ion number density and macroscopic velocity at infinity, respectively ($u_-^0 = -u$). It is assumed here that $m_- u^2/2 > e|\phi_0|$, where ϕ_0 is the soliton amplitude, so that there are no reflection of negative ions. The effects due to reflection of negative ions, when a finite temperature is considered for them, is expected to be small compared to the effects of reflected electrons, since $m_e/m_- << 1$.

In order to solve Eq. (1), a method similar to that described by Schamel (1972) will be used, in which the distribution functions $f_e(x',v)$ and $f_+(x',v)$ are prescribed and the potential $\phi(x')$ is calculated consistently using the Sagdeev potential formalism (Sagdeev, 1966). In this formalism, Eq. (1) is written in terms of the Sagdeev potential $V(\phi)$ as

$$\frac{d^2\phi(x')}{d(x')^2} = -\frac{1}{\varepsilon_0} \rho(x') \equiv -\frac{dV(\phi)}{d\phi} \ , \tag{8}$$

in analogy with the classical dynamics equation of motion for conservative systems, $md^2x/dt^2 = -dV/dx$. From (8), the Sagdeev potential can be expressed as

$$V(\phi) = V(0) + \frac{1}{\varepsilon_0} \int_0^{\phi} \rho(x') d\phi' \ . \tag{9}$$

This function must satisfy the conditions $V(\phi) = 0$ and $d\phi(x')/dx' = 0$, when $\phi = 0$ $(x' \to \pm\infty)$, which assure soliton type solutions (same behaviour of $V(\phi)$ at $x' \to \pm\infty$). Substituting the appropriate expressions for the particle charge densities in Eq. (9), yields an integral expression for $V(\phi)$.

The free particle distribution functions for both electrons and positive ions are considered to be shifted Maxwellians in the absence of reflected electrons and trapped positive ions. It is convenient to introduce at this point the following dimensionless variables: $\psi = -e\phi/k_B T_e$, $(\psi > 0)$, $\delta = m_e/m_+$, $U = u/C_+$ where $C_+ = (k_B T_e/m_+)^{1/2}$, $\theta_+ = T_+/T_e$, $\mu = m_-/m_+$ and $r = n_-^0/n_+^0$, where T_e is the electron temperature, T_+ is the positive ion temperature, k_B is Boltzmann's constant, n_+^0 and n_e^0 are the positive ion density and electron density at infinity, respectively. For the free electrons it is assumed

$$f_{ef}(x',v) = n_e^0\left(\frac{\delta}{2\pi}\right)^{1/2} \exp\left\{-\frac{\delta}{2}\left[U \pm \sqrt{v^2 - 2(\psi_0 - \psi)/\delta}\right]^2\right\}, \qquad (10)$$

where the (+) sign is used when $v > [2(\psi_0 - \psi)/\delta]^{1/2}$ and the (-) sign when $v < -[2(\psi_0 - \psi)/\delta]^{1/2}$. For the free positive ions,

$$f_{+f}(x',v) = n_+^0\left(\frac{1}{2\pi\theta_+}\right)^{1/2} \exp\left\{-\frac{1}{2\theta_+}\left[U \pm \sqrt{v^2 - 2\psi}\right]^2\right\}, \qquad (11)$$

where the (+) sign applies when $v > (2\psi)^{1/2}$ and the (-) sign when $v < -(2\psi)^{1/2}$.

The distribution functions for the reflected electrons and for the trapped positive ions are considered to be Maxwellian functions given, respectively, by

$$f_{er}(x',v) = n_e^0\left(\frac{\delta}{2\pi}\right)^{1/2}\exp\left(-\frac{\delta U^2}{2}\right)\exp\left\{-\alpha\left[\frac{\delta v^2}{2} - (\psi_0 - \psi)\right]\right\}, \qquad (12)$$

for $|v| \leq [2(\psi_0 - \psi)/\delta]^{1/2}$, and

$$f_{+t}(x',v) = n_+^0\left(\frac{1}{2\pi\theta_+}\right)^{1/2}\exp\left(-\frac{U^2}{2\theta_+}\right)\exp\left[-\frac{\beta}{2\theta_+}(v^2 - 2\psi)\right], \qquad (13)$$

for $|v| \leq (2\psi)^{1/2}$, where the parameters α and β are used to adjust the form of the distribution functions of the reflected electrons and the trapped positive ions, respectively, and are allowed to be negative as well, corresponding to a depression in the corresponding distribution functions. Note that the distribution functions f_e and f_+ are continuous at the points $v = \pm[2(\psi_0 - \psi)/\delta]^{1/2}$ and $v = \pm(2\psi)^{1/2}$, respectively. Fig. 1 illustrates qualitatively the form of the distribution functions for the electrons and for the positive ions, and the role played by the parameters α and β on the particle densities. Note that for $\alpha = 1$ the electron distribution function reduces to a Maxwellian, except in the velocity interval $-[U^2 + 2(\psi_0 - \psi)/\delta]^{1/2} \leq v \leq -[2(\psi_0 - \psi)/\delta]^{1/2}$.

Using these expressions for the distribution functions in the charge density equation (3), and introducing polar coordinates (r,θ) the integral in r can be performed analytically. After some mathematical manipulations, following the method used by Schamel (1972), the particle charge densities can be expressed as

$$\rho_e(x') = -e(1 - r)n_+^0 \left[\exp(\psi_0)\operatorname{erfc}(\sqrt{\psi_0}) + K\left(\frac{\delta U^2}{2}, \psi_0\right) + \right.$$

$$\left. + |\alpha|^{-1/2} \begin{cases} \exp(\alpha\psi_0)\operatorname{erf}(\sqrt{\alpha\psi_0}) \\ \frac{2}{\sqrt{\pi}} F(\sqrt{|\alpha|\psi_0}) \end{cases} \right]^{-1} \times \left[\exp(\psi_0 - \psi)\operatorname{erfc}(\sqrt{\psi_0 - \psi}) + \right.$$

$$\left. + K\left(\frac{\delta U^2}{2}, \psi_0 - \psi\right) + |\alpha|^{-1/2} \begin{cases} \exp[\alpha(\psi_0 - \psi)]\operatorname{erf}(\sqrt{\alpha(\psi_0 - \psi)}) \\ \frac{2}{\sqrt{\pi}} F[\sqrt{|\alpha|(\psi_0 - \psi)}] \end{cases} \right] \begin{matrix} \alpha \geq 0 \\ \alpha < 0 \end{matrix} \qquad (14)$$

and

$$\rho_+(x') = en_+^0 \exp\left(-\frac{U^2}{2\theta_+}\right) \left[\exp\left(\frac{\psi}{\theta_+}\right)\operatorname{erfc}\left(\sqrt{\frac{\psi}{\theta_+}}\right) + K\left(\frac{U^2}{2\theta_+}, \frac{\psi}{\theta_+}\right) + \right.$$

$$\left. + |\beta|^{-1/2} \begin{cases} \exp\left(\frac{\beta\psi}{\theta_+}\right)\operatorname{erf}\left(\sqrt{\frac{\beta\psi}{\theta_+}}\right) \\ \frac{2}{\sqrt{\pi}} F\left(\sqrt{\frac{|\beta|\psi}{\theta_+}}\right) \end{cases} \right] \begin{matrix} \beta \geq 0 \\ \beta < 0 \end{matrix} . \qquad (15)$$

For the negative ions, from Eq. (5),

$$\rho_-(x') = -\frac{ern_+^0}{(1 - 2\psi/\mu U^2)^{1/2}} . \qquad (16)$$

In these expressions the quantities n_e^0 and n_-^0 have been eliminated using the macroscopic charge neutrality condition at $x' \to \infty$ ($\psi = 0$),

$$\lim_{\psi \to 0} \Sigma \rho_a(x') = 0 \ . \tag{17}$$

The integral K(a,b) is defined as

$$K(a,b) = 2\sqrt{\frac{a}{\pi}} \int_0^{\pi/2} d\theta \cos\theta \exp(a\cos^2\theta - b\,\mathrm{tg}^2\theta)\mathrm{erf}(\sqrt{a}\cos\theta) \ , \tag{18}$$

the function F(x) is the Dawson integral

$$F(x) = \exp(-x^2) \int_0^x \exp(t^2)dt \ , \tag{19}$$

erf(x) is the error function

$$\mathrm{erf}(x) = \frac{2}{\sqrt{\pi}} \int_0^x \exp(-t^2)dt \ , \tag{20}$$

and erfc(x) is the complementary error function erfc(x) = 1 - erf(x). These integrals must be solved numerically.

Poisson equation (8) in normalized form becomes

$$\left(\frac{\lambda_e}{\ell}\right)^2 \frac{d^2\psi(\xi)}{d\xi^2} = - \frac{dV(\psi)}{d\psi} \ , \tag{21}$$

where $\xi = x'/\ell$, with ℓ a scale length associated with spatial gradients and λ_e is the Debye length

$$\lambda_e^2 = \frac{\varepsilon_0 k_B T_e}{e^2(1 - r)n_+^0} \ . \tag{22}$$

The normalized Sagdeev potential is therefore given by

$$V(\psi) = \frac{1}{\rho_e^0} \int_0^{\psi} [\rho_e(\psi') + \rho_+(\psi') + \rho_-(\psi')]d\psi' \ , \tag{23}$$

with the charge densities given by Eqs. (14), (15) and (16).

In order to obtain a relationship between the soliton amplitude ψ_0 and its velocity $U(\psi_0)$, the equation $V(\psi_0) = 0$ is considered next. After some mathematical manipulations it is obtained from (23) (for details refer to Roberto, 1986),

$$V(\psi_0) = \left[\exp(\psi_0)\mathrm{erfc}(\sqrt{\psi_0}) + K\left(\frac{\delta U^2}{2} \ , \ \psi_0\right) + \right.$$

$$\left. + |\alpha|^{-1/2} \left\{ \begin{array}{l} \exp(\alpha\psi_0)\mathrm{erf}(\sqrt{\alpha\psi_0}) \\ \\ \frac{2}{\sqrt{\pi}} F(\sqrt{|\alpha|\psi_0}) \end{array} \right\} \right]^{-1} \times$$

$$\times \left[\exp(\psi_0)\mathrm{erfc}(\sqrt{\psi_0}) + \frac{2}{\sqrt{\pi}}\sqrt{\psi_0} - 1 + H\left(\frac{\delta U^2}{2} \ , \ 0 \ , \ \psi_0\right) + \right.$$

$$\left. + \frac{|\alpha|^{-1/2}}{\alpha} \left\{ \begin{array}{l} \exp(\alpha\psi_0)\mathrm{erf}(\sqrt{\alpha\psi_0}) - \frac{2}{\sqrt{\pi}}\sqrt{\alpha\psi_0} \\ \\ \frac{2}{\sqrt{\pi}} F(\sqrt{|\alpha|\psi_0}) - \frac{2}{\sqrt{\pi}}\sqrt{|\alpha|\psi_0} \end{array} \right\} \right] +$$

$$+\frac{r\mu U^2}{(1-r)}\left(1-\sqrt{1-\frac{2\psi_0}{\mu U^2}}\right)-\frac{\theta_+}{(1-r)}\exp\left(-\frac{U^2}{2\theta_+}\right)\times$$

$$\times\left[\exp\left(\frac{\psi_0}{\theta_+}\right)\operatorname{erfc}\left(\sqrt{\frac{\psi_0}{\theta_+}}\right)+\frac{2}{\sqrt{\pi}}\sqrt{\frac{\psi_0}{\theta_+}}-1+H\left(\frac{U^2}{2\theta_+},0,\frac{\psi_0}{\theta_+}\right)+\right.$$

$$\left.+\frac{|\beta|^{-1/2}}{\beta}\left\{\begin{array}{l}\exp\left(\frac{\beta\psi_0}{\theta_+}\right)\operatorname{erf}\left(\sqrt{\frac{\beta\psi_0}{\theta_+}}\right)-\frac{2}{\sqrt{\pi}}\sqrt{\frac{\beta\psi_0}{\theta_+}}\\ \\ \frac{2}{\sqrt{\pi}}F\left(\sqrt{\frac{|\beta|\psi_0}{\theta_+}}-\frac{2}{\sqrt{\pi}}\sqrt{\frac{|\beta|\psi_0}{\theta_+}}\right)\end{array}\right.\right]=0\qquad\begin{array}{l}\alpha,\beta\geq 0\\ \\ \alpha,\beta<0\end{array}\qquad(24)$$

where

$$H(a,b,c)=\int_b^c K(a,x)dx\ . \qquad (25)$$

3. LIMIT OF SMALL AMPLITUDES

In the limit of small amplitudes (when $\psi_0 \to 0$) Eq. (24) yields an expression for the normalized ion-acoustic velocity $S = C_s^{\sim}/C_+$. Expanding Eq. (24) in powers of ψ_0, for small ψ_0, and neglecting the inertia of electrons ($\delta = 0$), it is obtained

$$V(\psi_0)=\frac{\psi_0^2}{2}\left[A(U)+2\psi_0^{1/2}B(U)+\frac{1}{3}\psi_0 C(U)\right]=0\ , \qquad (26)$$

where

$$A(U)=-1+\frac{r}{(1-r)\mu U^2}-\frac{1}{(1-r)}\left[\frac{1}{\theta_+}-\frac{2}{\theta_+}\sqrt{\frac{U^2}{2\theta_+}}F\left(\sqrt{\frac{U^2}{2\theta_+}}\right)\right]\ , \qquad (27)$$

$$B(U) = -\frac{4}{5\sqrt{\pi}}(a-1) - \frac{8}{15\sqrt{\pi}(1-r)}\exp\left(-\frac{U^2}{2\theta_+}\right)\frac{1}{\theta_+^{3/2}}\left(\beta - 1 + \frac{U^2}{\theta_+}\right), \quad (28)$$

and

$$C(U) = 1 + \frac{3r}{(1-r)\mu^2U^4} + \frac{1}{(1-r)}\left[-\frac{1}{\theta_+^2} + \frac{U^2}{2\theta_+^3} + \right.$$

$$\left. + \left(3 - \frac{U^2}{\theta_+}\right)\sqrt{\frac{U^2}{2\theta_+}}\,F\left(\sqrt{\frac{U^2}{2\theta_+}}\right)\frac{1}{\theta_+^2}\right]. \quad (29)$$

In the limit $\psi_0 \to 0$ (i.e. $U = S$) Eq. (26) leads to $A(S) = 0$, which gives the following expression

$$-1 + \frac{r}{(1-r)\mu S^2} - \frac{1}{(1-r)}\left[\frac{1}{\theta_+} - \frac{2}{\theta_+}\sqrt{\frac{S^2}{2\theta_+}}\,F\left(\sqrt{\frac{S^2}{2\theta_+}}\right)\right] = 0. \quad (30)$$

When $\theta_+ \to 0$ this equation must yield an expression for S identical to that obtained from the fluid model. Using an asymptotic expansion for the Dawson integral, when $\theta_+ \to 0$, it is obtained accordingly,

$$S = \left(\frac{1 + r/\mu}{1 - r}\right)^{1/2}. \quad (31)$$

For arbitrary values of θ_+, Eq. (30) must be solved numerically.

The Mach number $M = U/S$ can also be expanded in terms of powers of ψ_0, in the small amplitude limit, so that it can be written approximately as

$$M \simeq 1 + b\psi_0^{1/2} + c\psi_0, \quad (32)$$

where b and c are constants. As r increases ($r \geq 0.10$), $\theta_+ \to 0$ and $\alpha = 1$, b becomes negligible (Roberto, 1986) and Eq. (32) reduces to

$$M = 1 + c\psi_0 \quad . \tag{33}$$

4. RESULTS AND DISCUSSION

Numerical values for the normalized ion-acoustic velocity S, and for the soliton velocity U, can be obtained from Eqs. (30) and (24), respectively. Solutions with U > S must be considered since the solitons can propagate only with velocities above the ion-acoustic velocity. Using this approach, numerical values can be determined for the Mach number M = U/S as a function of ψ_0, for given values of r, μ, θ_+, α and β. For purposes of comparison with the experimental observations of Ludwig et al. (1984) and Nakamura et al. (1985a) it is considered here specifically a plasma composed of Ar^+ and F^-.

Initially, in order to investigate the kinetic effect due to the trapping of positive ions on the soliton velocity, Eqs. (24) and (30) are considered in the limit when $\delta = 0$ and $\alpha = 1$ (neglecting for the moment the effect due to reflection of electrons). A plot of the coefficient $-c = -(M - 1)/\psi_0$ versus concentration r, for various values of θ_+ and with $\beta = 1$, is shown in Fig. 2, for purposes of comparison with Fig. 1 of Ludwig et al. (1984) and Fig. 6 of Nakamura et al. (1985a). The principal effect associated with the finite temperature, and trapping, of the Ar^+ ions is a reduction in the soliton velocity as θ_+ increases, for a given amplitude and concentration r. As the positive ion temperature increases, the corresponding distribution function

becomes broader, so that more ions are available with sufficiently low energy to become trapped in the soliton potential well. The numerical results also show that small changes in the parameter β have little effect on the soliton velocity, for a given temperature θ_+. This result is in contrast to that obtained by Nakamura et al. (1985a) (the dashed curve of their Fig. 6) using a fluid model, who concluded that the soliton velocity increases as the positive ion temperature increases, a result analogous to that obtained by Sakanaka (1972) for positive solitons. This difference in behaviour may be due to the inclusion, in the kinetic model, of positive ion trapping in the soliton potential well, which causes a decrease in the soliton velocity. Similar behaviour was obtained by Schamel (1979), analyzing the effect of electron trapping in a positive soliton, who concluded that, as the population of trapped electrons increases, the soliton velocity decreases. From the curves in Fig. 2 the minimum critical concentration r_c necessary to have negative soliton solutions can be estimated, noting that as θ_+ increases, a larger amount of F^- is required.

In order to show the effect due to reflection of electrons by the soliton potential well, it is presented in Figs. 3, 4, 5 and 6 plots of the Mach number $M = U/S$ as function of the soliton amplitude ψ_0, for $r = 0.15$, 0.26, 0.35 and 0.62, respectively, considering various values of α and for $\theta_+ = 0$ (neglecting for the moment the effect of positive ion trapping). The experimental values obtained in a double-plasma machine by Ferreira (1986) are also shown, for purposes of comparison. It is seen the population of reflected electrons, represented by the parameter α, has a large effect on the soliton velocity. For a given

amplitude, as α decreases (representing a decrease in the amount of reflected electrons), the soliton velocity increases, so that for a given concentration r there is a value of α which best fits the experimental values. Note also that, for a given ψ_0 and α, the dependence of M on r reaches a maximum at a given concentration. This behaviour is also evident in the experimental data of Ferreira (1986) and Ludwig (1984).

Fig. 7 shows M versus ψ_0 for various values of θ_+, considering $\beta = 1$, $r = 0.26$ and $\alpha = 0.20$, to illustrate the kinetic effect of positive ion trapping, relative to that of electron reflection. It is seen that for a given α and r, M decreases as θ_+ increases. For $\alpha = 1$ and $\theta_+ = 0$ the results reproduce those predicted by the fluid model.

The effects of ion trapping and electron reflection on the soliton amplitude can be physically understood by looking at the negative soliton spatial charge distribution shown in Fig. 8. Reflected electrons of high energy spend more time close to the soliton center enhancing the negative charge at the potential well, while low energy electrons reduce the positive charge density at the wings of the structure. Therefore, depending on the value of α, reflected electrons can increase or decrease the soliton amplitude. On the other hand, the positive trapped ions will reduce the negative space charge in the potential well, decreasing the soliton amplitude.

The results presented indicate that the experimental values obtained for M can be reproduced by proper selection of the parameters α and θ_+, which may vary for different concentrations. For $r = 0.35$ (Fig. 5), for example, negative values of α are required to explain the relatively large experimental values of M, which suggest the existence of a

depression in the distribution function for the reflected electrons. Yoshizawa et al. (1979) have investigated theoretically the form of the electron distribution function in a plasma of SF_6, showing that there are energy ranges in which electrons are removed from the plasma due to electron attachment to form the negative ions. In the low energy range ($\leq$1eV), corresponding to that in which electron reflection occurs, the cross sections for capture of electrons to form SF_5^- and SF_6^- are large [Fig. 1 of Yoshizawa et al. (1979)], suggesting the existence of a depression in the electron distribution function in this energy range. These considerations are consistent with the numerical results presented here, which show that as r increases (increasing the amount of SF_6 in the chamber), a smaller amount of reflected electrons (α) is required to fit the experimental data, up to a certain value of r. However, above a given value of r, M starts to decrease, as can be seen from Fig. 6 for r = 0.62. As r increases, less electrons are available in the plasma, and as r $\rightarrow$ 1 (limiting case in which the plasma neutrality is due to F^- only) the theoretical as well as experimental values found for M must tend to the same value as predicted by the fluid model. However, it is found here that for large r ($r \geq 0.50$), the experimental values approach this limiting value faster than the theoretical ones. This means that increasingly larger α values are necessary to explain the experimental data as r increases ($r \geq 0.50$). Although this result apparently contradicts the previous argument used to explain the depression in the distribution function of reflected electrons for small values of r (α must decrease as r increases, when $r \leq 0.50$), it may be related to a reduction in the r lative concentration of SF_5^- and SF_6^-,

since as r increases, the F^- ion concentration becomes dominant, as suggested by Ludwig et al. (1984).

5. SUMMARY AND CONCLUSIONS

The role played by positive ion trapping and electron reflection on the propagation characteristics of negative solitons, has been investigated using a kinetic model, considering specifically a plasma produced from a mixture of Ar and SF_6. The particle distribution functions have been prescribed and the soliton electric potential determined consistently using the Sagdeev potential formalism. The numerical results obtained are compared with experimental data measured in the multicomponent plasma produced in a double plasma machine. It is found that the experimental data for the soliton propagation velocity can be reproduced by proper selection of the particle distribution functions, for given plasma parameters. The population of reflected electrons and trapped positive ions play an important role on the soliton propagation velocity, and the results show that the soliton velocity decreases as the population of reflected electrons and trapped positive ions increases, for a given concentration and soliton amplitude. Adjusting properly the parameters α and θ_+, for a given concentration, the experimental values for M can be satisfactorily reproduced. Measurements of the particle distribution functions seem therefore to be very important for understanding the kinetic effects on the propagation characteristics of negative solitons and for the development of a kinetic model.

FIGURE CAPTIONS

Fig. 1 - Form of the distribution fucntions for electrons and ions indicating the effect of the parameters α and β on the densities of the reflected electrons and trapped positive ions.

Fig. 2 - Dependence of $-(M - 1)/\psi_0$ on the concentration ratio $r = n_-^0/n_+^0$, illustrating the kinetic effect due trapping of positive ions, for $\beta = 1$ and $\theta_+ = 0$, 1/15, 1/10, 1/8, 1/5.

Fig. 3 - Dependence of the Mach numer M on the amplitude ψ_0, for $r = 0.15$, $\theta_+ = 0$ and various values of α, showing the effect of the reflected electrons.

Fig. 4 - Same as in Fig. 3, but for $r = 0.26$.

Fig. 5 - Same as in Fig. 3, but for $r = 0.35$.

Fig. 6 - Same as in Fig. 3, but for $r = 0.62$.

Fig. 7 - Dependence of the Mach number M on the amplitude $\tilde{\psi}_0$, for $r = 0.26$, $\alpha = 0.20$ and various values of θ_+, showing the effects due to electron reflection and positive ion trapping.

Fig. 8 - Space charge distribution in a negative soliton.

REFERENCES

DAS G.C. and TAGARE S.G. (1975) Plasma Phys. 17, 1025.

FERREIRA J.L. Dissertation (1986), Report 4100-TDL/257, INPE. Published in Portuguese.

IKEZI H., TAYLOR R.J. and BAKER D.R. (1970) Phys. Rev. Lett. 25, 11.

LUDWIG G.O., FERREIRA J.L. and NAKAMURA, Y. (1984) Phys. Rev. Lett. 52, 275.

NAKAMURA Y. and TSUKABAYASHI I. (1984) Phys. Rev. Lett. 52, 2356.

NAKAMURA Y., FERREIRA J.L. and LUDWIG G.O. (1985a) 33, 237.

NAKAMURA Y., TSUKABAYASHI I., LUDWIG G.O. and FERREIRA J.L. (1985b) Phys. Lett. 113A, 155.

ROBERTO M. Thesis (1986), Report 4092-TDL/253, INPE. Published in Portuguese.

SAGDEEV R.Z., Reviews of plasma physics, Vol. 4 (Consultants Bureau, New York, 1966).

SAKANAKA P.H. (1972) Phys. Fluids 15, 304.

SCHAMEL H. (1972) Plasma Phys. 14, 905.

SCHAMEL H. (1973) Plasma Phys. 9, 377.

SCHAMEL H. (1979) Phys. Scr. 20, 306.

TAGARE S.G. (1975) J. Plasma Phys. 14, 1.

TRAN M.Q. (1979) Phys. Scr. 20, 317.

WASHIMI H. and TANIUTI T. (1966) Phys. Rev. Lett. 17, 996.

YOSHIZAWA T., SAKAI Y., TAGASHIRA, H. and SAKAMOTO S. (1979) J. of Phys. D: Applied Phys. 12, 1839.

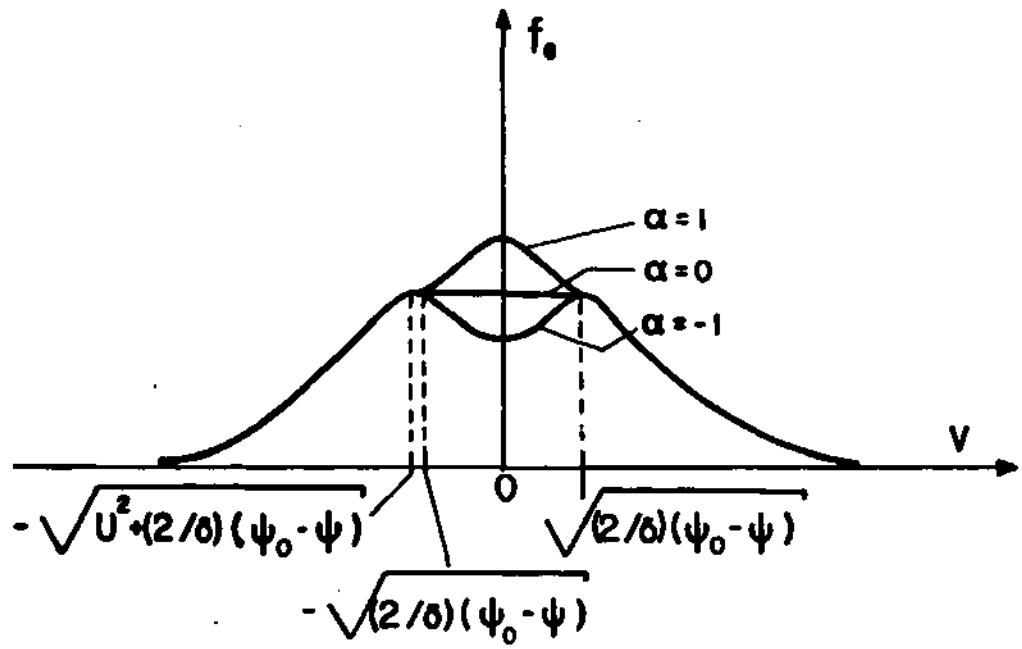
f_e
$\alpha = 1$
$\alpha = 0$
$\alpha = -1$
V
0
$-\sqrt{U^2+(2/\delta)(\psi_0-\psi)}$
$\sqrt{(2/\delta)(\psi_0-\psi)}$
$-\sqrt{(2/\delta)(\psi_0-\psi)}$

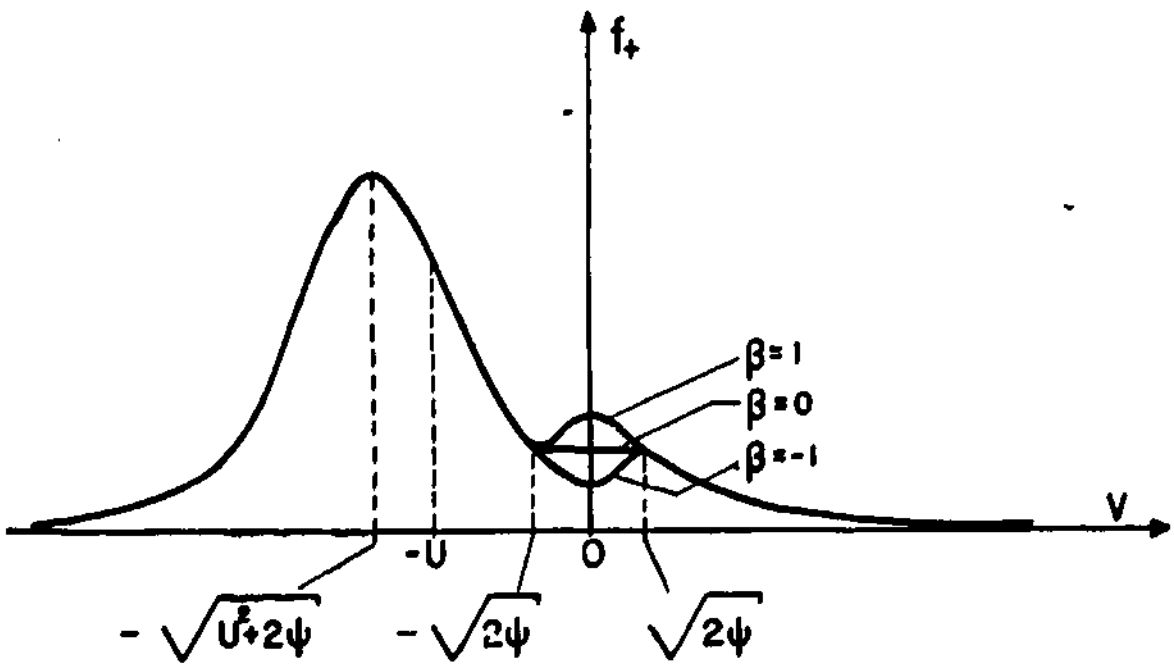
f_+
$\beta = 1$
$\beta = 0$
$\beta = -1$
V
-U
0
$-\sqrt{U^2+2\psi}$
$-\sqrt{2\psi}$
$\sqrt{2\psi}$

Fig. 1

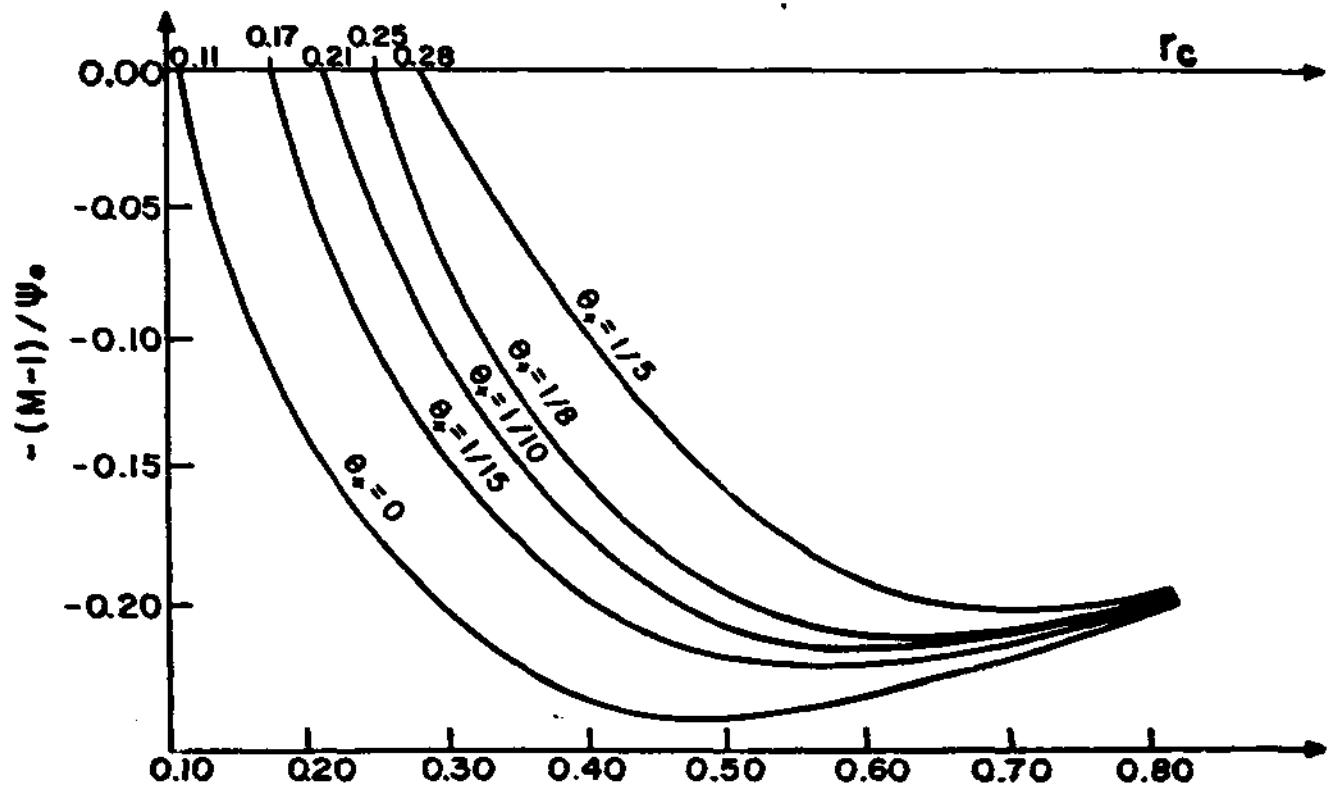
0.11
0.17
0.21
0.25
0.28
r_c
0.00
-0.05
-0.10
-0.15
-0.20
$-(M-1)/\psi_\bullet$
$\theta_\bullet = 1/5$
$\theta_\bullet = 1/8$
$\theta_\bullet = 1/10$
$\theta_\bullet = 1/15$
$\theta_\bullet = 0$
0.10
0.20
0.30
0.40
0.50
0.60
0.70
0.80
CONCENTRATION RATIO r

Fig. 2

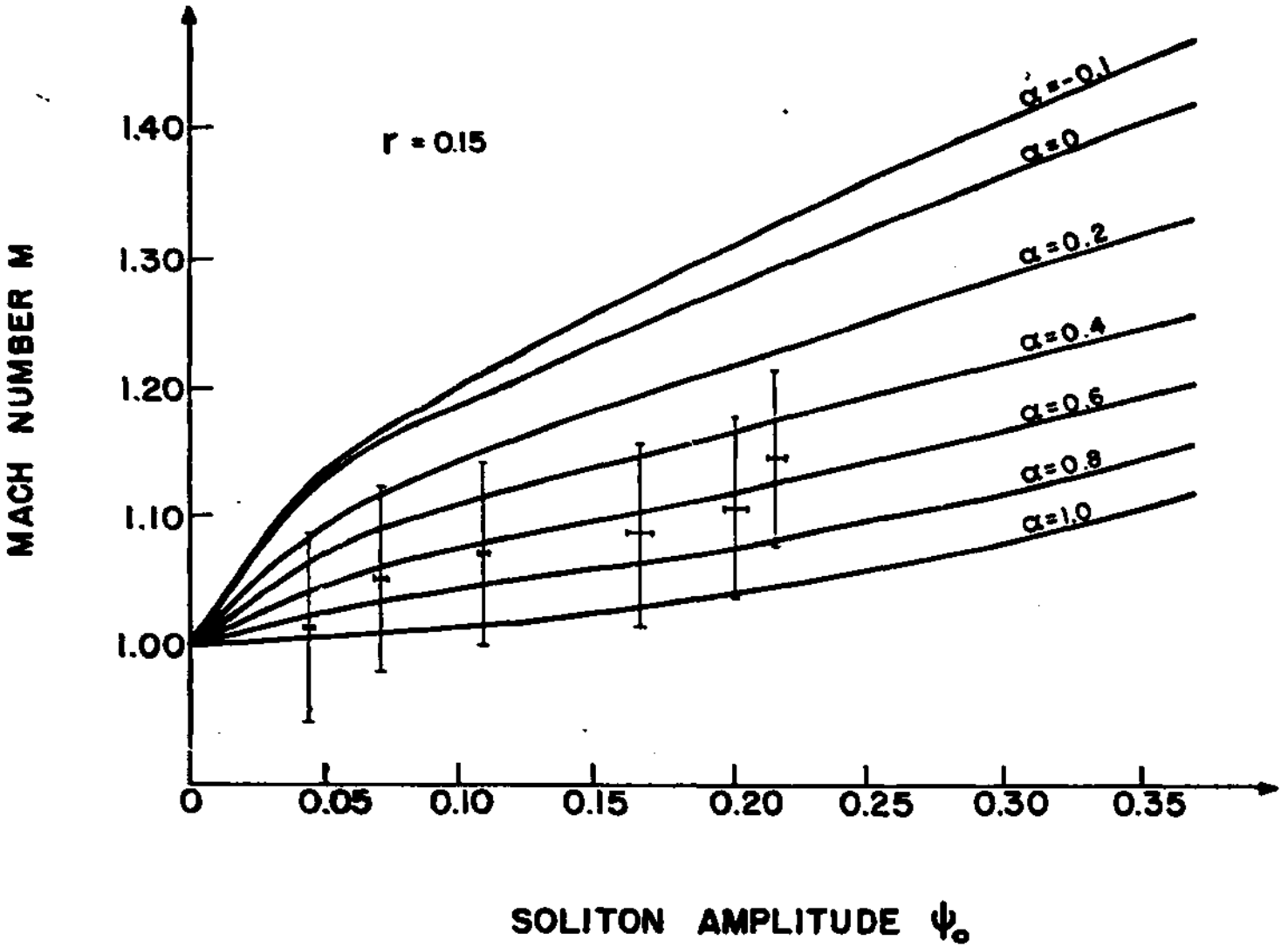
MACH NUMBER M
1.40
1.30
1.20
1.10
1.00
r = 0.15
α=-0.1
α=0
α=0.2
α=0.4
α=0.6
α=0.8
α=1.0
0
0.05
0.10
0.15
0.20
0.25
0.30
0.35
SOLITON AMPLITUDE ψ₀

Fig. 3

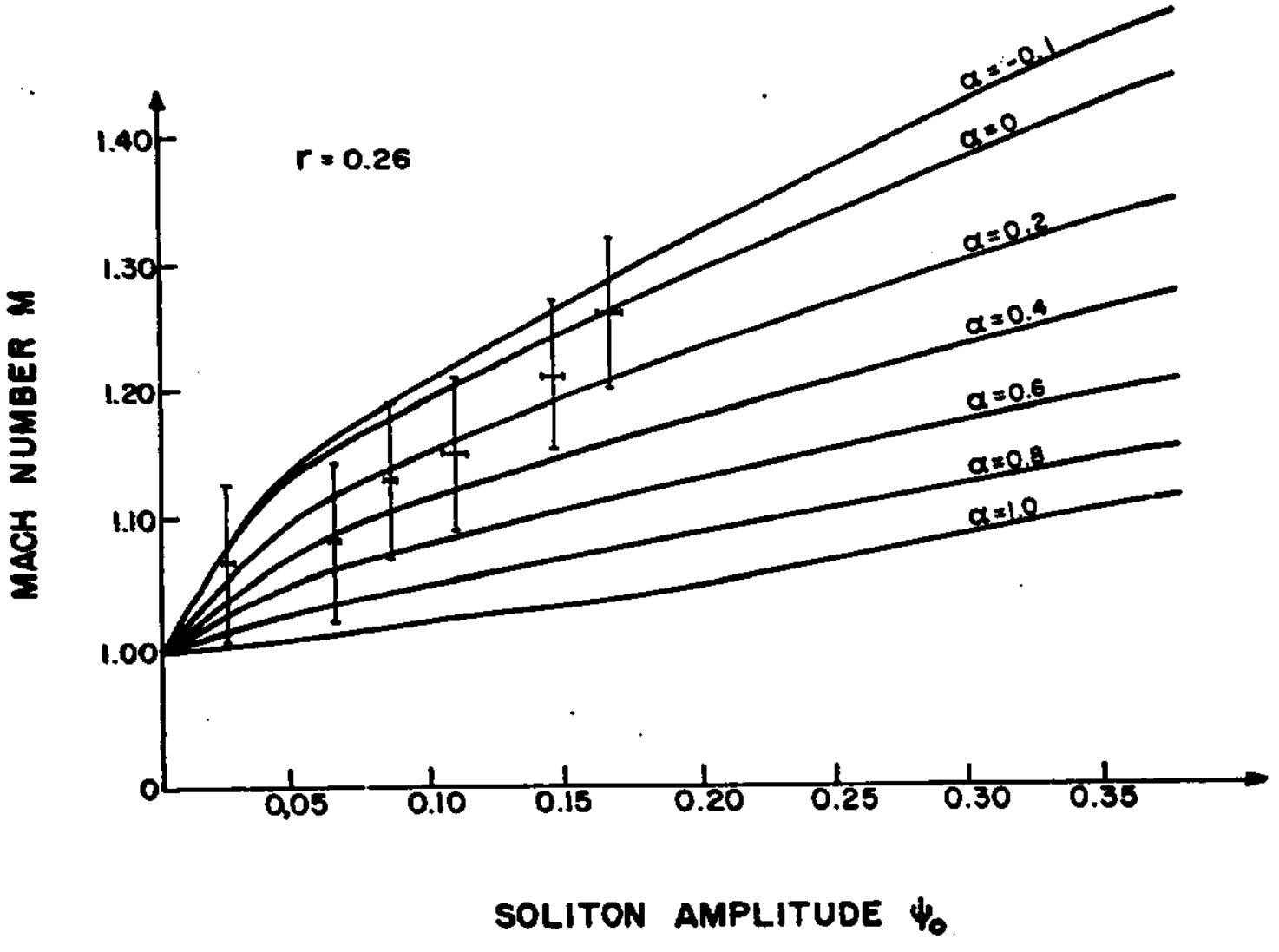
MACH NUMBER M
1.40
1.30
1.20
1.10
1.00
0
r = 0.26
α = -0.1
α = 0
α = 0.2
α = 0.4
α = 0.6
α = 0.8
α = 1.0
0.05
0.10
0.15
0.20
0.25
0.30
0.35
SOLITON AMPLITUDE ψ₀

Fig. 4

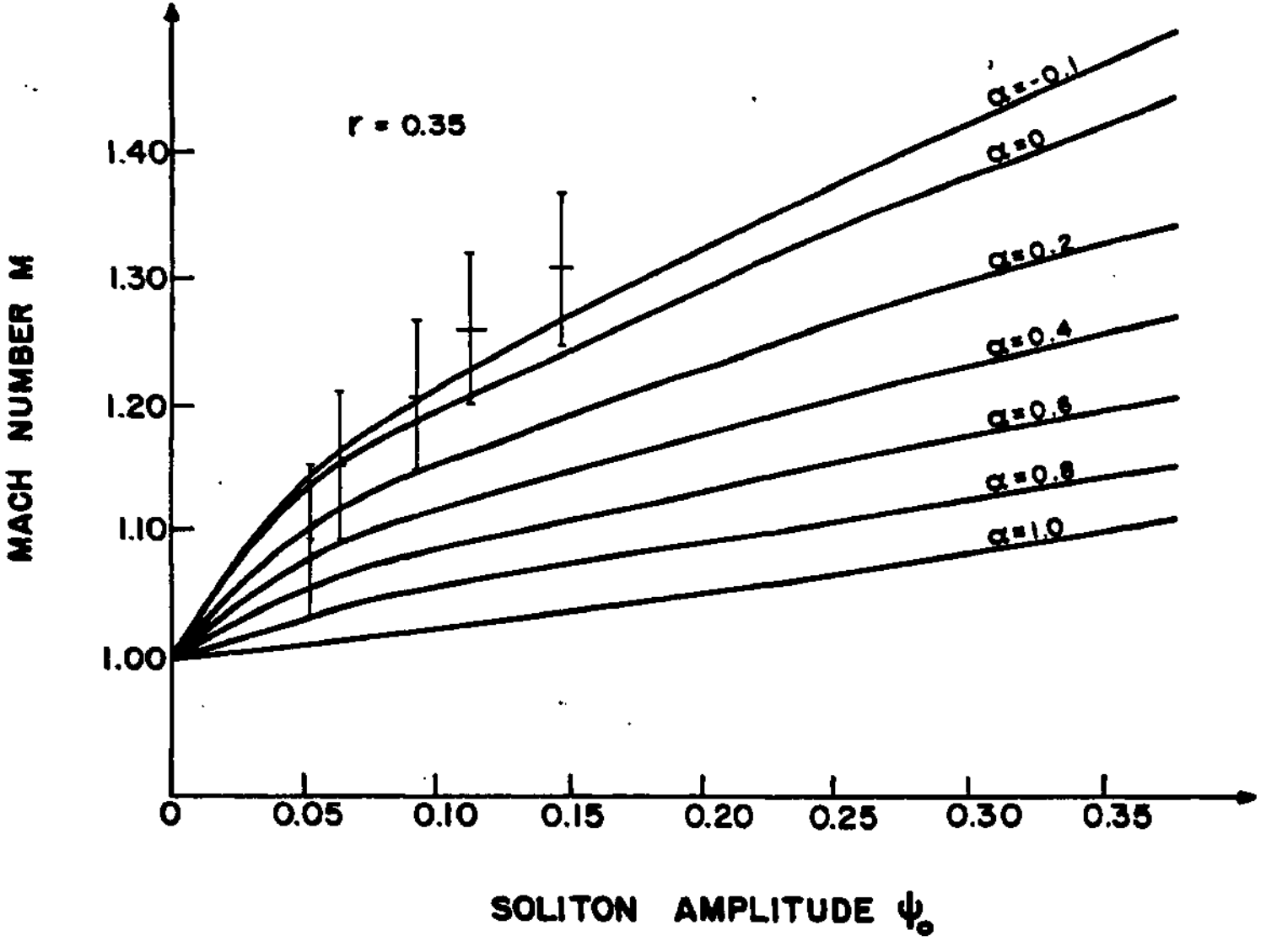
r = 0.35
α=-0.1
α=0
α=0.2
α=0.4
α=0.6
α=0.8
α=1.0
MACH NUMBER M
1.00
1.10
1.20
1.30
1.40
0
0.05
0.10
0.15
0.20
0.25
0.30
0.35
SOLITON AMPLITUDE ψ₀

Fig. 5

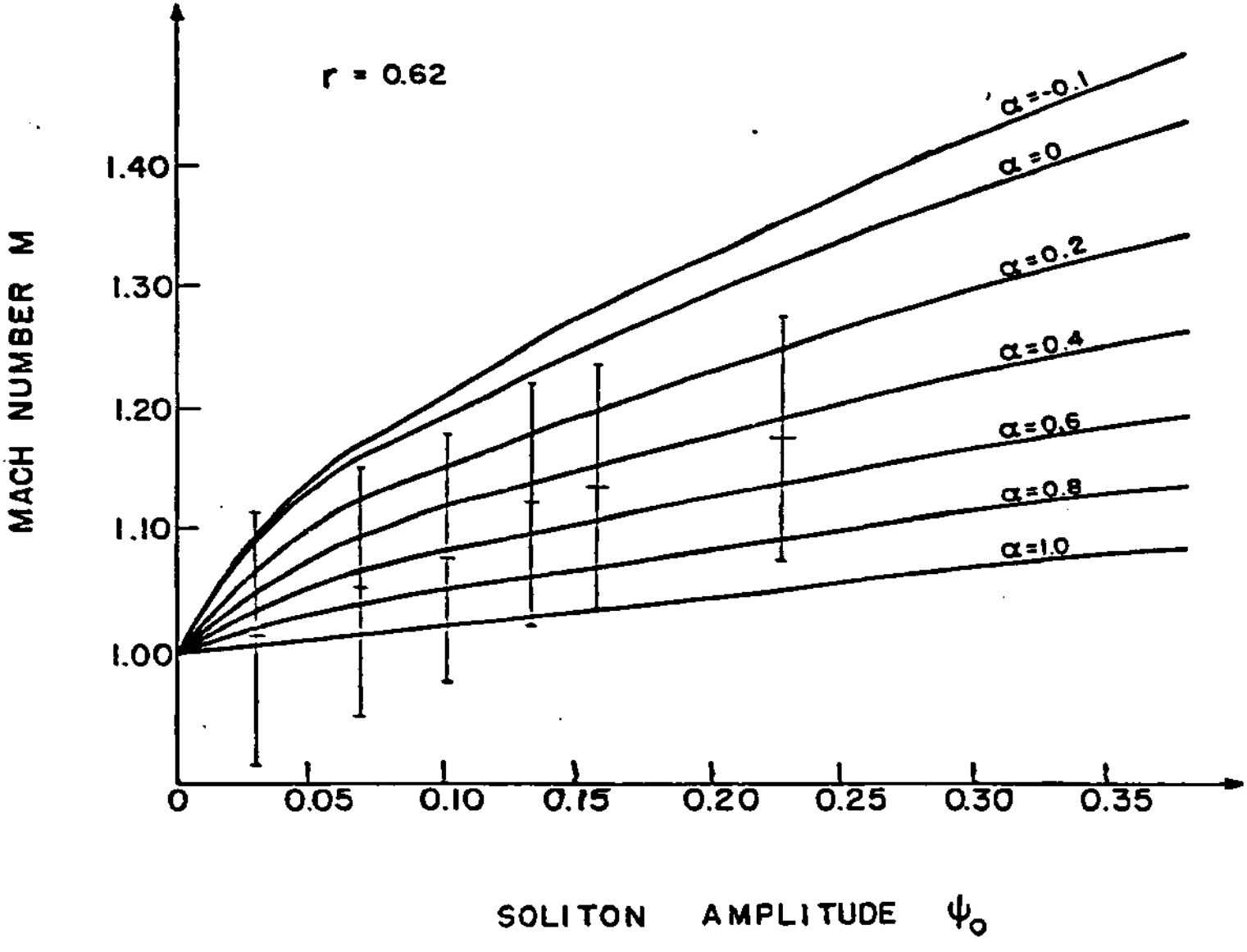
r = 0.62
α=-0.1
α=0
α=0.2
α=0.4
α=0.6
α=0.8
α=1.0
1.40
1.30
1.20
1.10
1.00
MACH NUMBER M
0
0.05
0.10
0.15
0.20
0.25
0.30
0.35
SOLITON AMPLITUDE ψ_0

Fig. 6

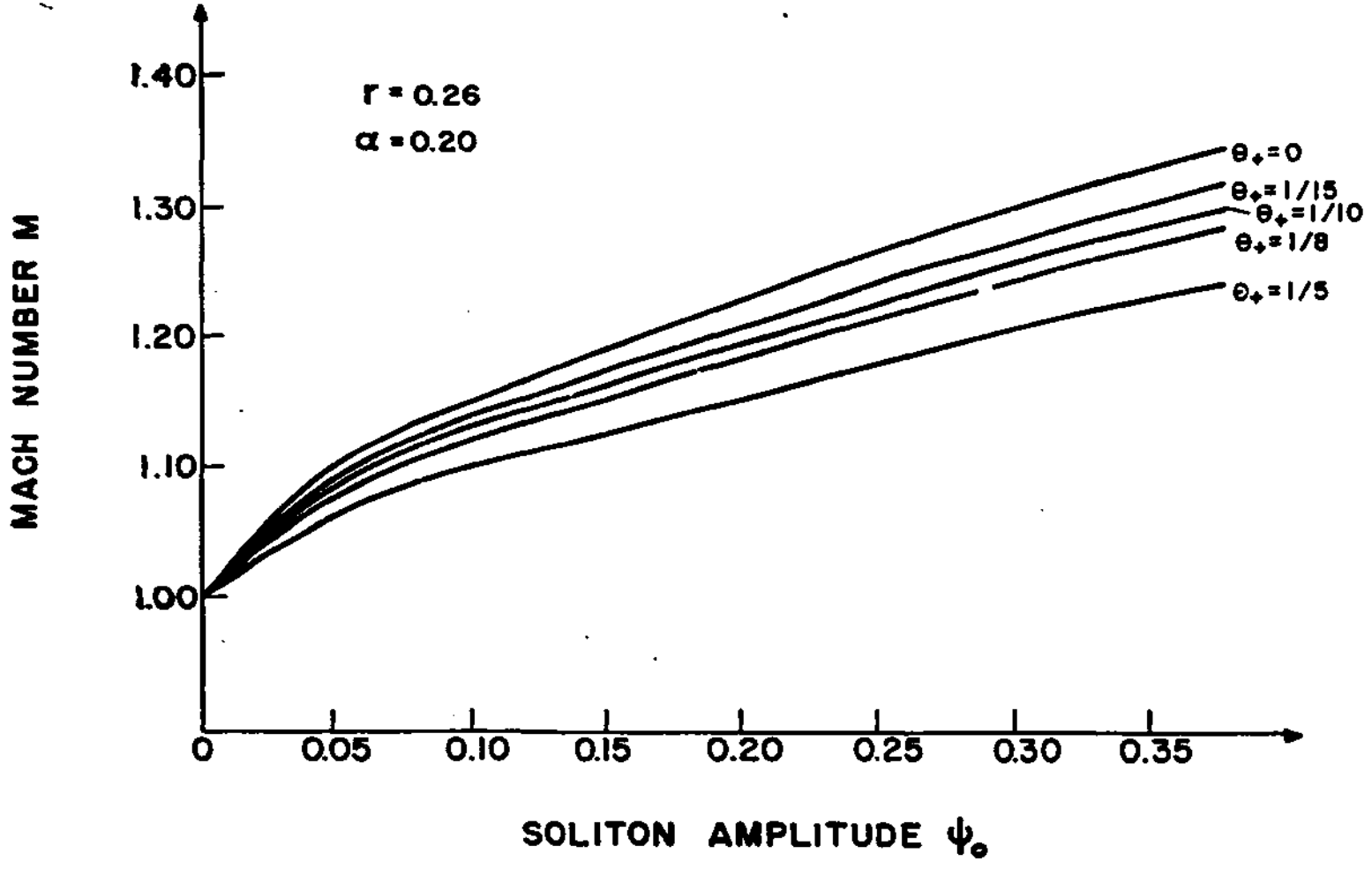
MACH NUMBER M
1.40
1.30
1.20
1.10
1.00
r = 0.26
α = 0.20
θ+ = 0
θ+ = 1/15
θ+ = 1/10
θ+ = 1/8
θ+ = 1/5
0
0.05
0.10
0.15
0.20
0.25
0.30
0.35
SOLITON AMPLITUDE ψo

Fig. 7

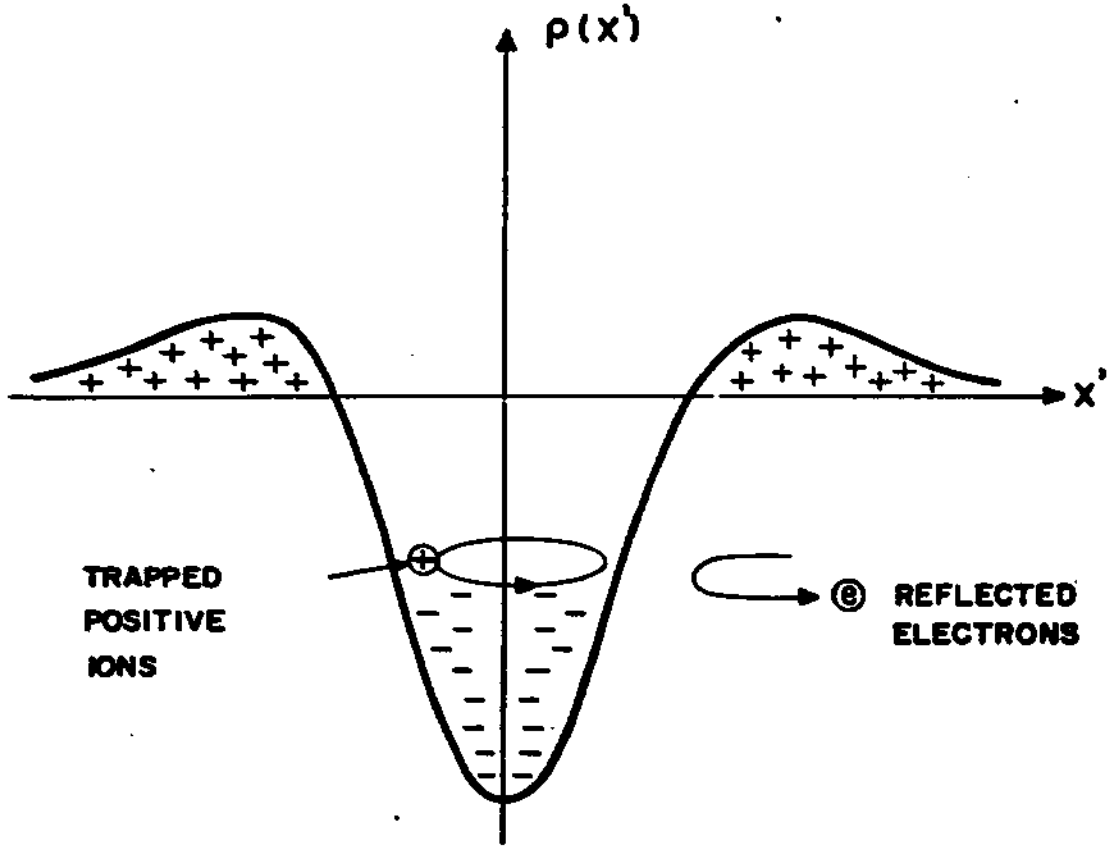

Fig. 8